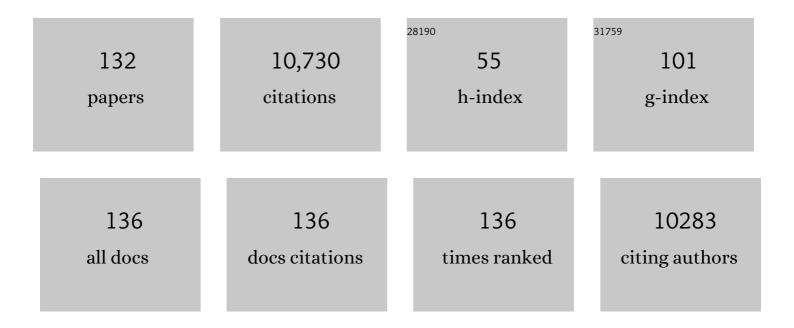
Kui Zhao

List of Publications by Year in descending order

Source: https://exaly.com/author-pdf/2083159/publications.pdf Version: 2024-02-01



<u>Кш 7нло</u>

#	Article	IF	CITATIONS
1	Ligand-Stabilized Reduced-Dimensionality Perovskites. Journal of the American Chemical Society, 2016, 138, 2649-2655.	6.6	1,157
2	Stable Highâ€Performance Perovskite Solar Cells via Grain Boundary Passivation. Advanced Materials, 2018, 30, e1706576.	11.1	665
3	Stable high efficiency two-dimensional perovskite solar cells via cesium doping. Energy and Environmental Science, 2017, 10, 2095-2102.	15.6	588
4	Precursor Engineering for Allâ€inorganic CsPbI ₂ Br Perovskite Solar Cells with 14.78% Efficiency. Advanced Functional Materials, 2018, 28, 1803269.	7.8	264
5	A 1300 mm ² Ultrahighâ€Performance Digital Imaging Assembly using Highâ€Quality Perovskite Single Crystals. Advanced Materials, 2018, 30, e1707314.	11.1	246
6	Phase Transition Control for High Performance Ruddlesden–Popper Perovskite Solar Cells. Advanced Materials, 2018, 30, e1707166.	11.1	244
7	Solutionâ€Processed Small Moleculeâ€Polymer Blend Organic Thinâ€Film Transistors with Hole Mobility Greater than 5 cm ² /Vs. Advanced Materials, 2012, 24, 2441-2446.	11.1	219
8	Multi-inch single-crystalline perovskite membrane for high-detectivity flexible photosensors. Nature Communications, 2018, 9, 5302.	5.8	212
9	Surface-Tension-Controlled Crystallization for High-Quality 2D Perovskite Single Crystals for Ultrahigh Photodetection. Matter, 2019, 1, 465-480.	5.0	202
10	Holeâ€Transporting Transistors and Circuits Based on the Transparent Inorganic Semiconductor Copper(I) Thiocyanate (CuSCN) Processed from Solution at Room Temperature. Advanced Materials, 2013, 25, 1504-1509.	11.1	196
11	High performance ambient-air-stable FAPbI ₃ perovskite solar cells with molecule-passivated Ruddlesden–Popper/3D heterostructured film. Energy and Environmental Science, 2018, 11, 3358-3366.	15.6	196
12	Dynamical Transformation of Two-Dimensional Perovskites with Alternating Cations in the Interlayer Space for High-Performance Photovoltaics. Journal of the American Chemical Society, 2019, 141, 2684-2694.	6.6	189
13	Phase Transition Control for High-Performance Blade-Coated Perovskite Solar Cells. Joule, 2018, 2, 1313-1330.	11.7	180
14	Fine Multiâ€Phase Alignments in 2D Perovskite Solar Cells with Efficiency over 17% via Slow Postâ€Annealing. Advanced Materials, 2019, 31, e1903889.	11.1	178
15	Blade-Coated Hybrid Perovskite Solar Cells with Efficiency > 17%: An In Situ Investigation. ACS Energy Letters, 2018, 3, 1078-1085.	8.8	171
16	Compositional Control in 2D Perovskites with Alternating Cations in the Interlayer Space for Photovoltaics with Efficiency over 18%. Advanced Materials, 2019, 31, e1903848.	11.1	171
17	Electric field-induced hole transport in copper(i) thiocyanate (CuSCN) thin-films processed from solution at room temperature. Chemical Communications, 2013, 49, 4154-4156.	2.2	169
18	Spin ast Bulk Heterojunction Solar Cells: A Dynamical Investigation. Advanced Materials, 2013, 25, 1923-1929.	11.1	163

#	Article	IF	CITATIONS
19	Interfacial Engineering at the 2D/3D Heterojunction for High-Performance Perovskite Solar Cells. Nano Letters, 2019, 19, 7181-7190.	4.5	163
20	Tripleâ€Cation and Mixedâ€Halide Perovskite Single Crystal for Highâ€Performance Xâ€ray Imaging. Advanced Materials, 2021, 33, e2006010.	11.1	163
21	Printable CsPbI ₃ Perovskite Solar Cells with PCE of 19% via an Additive Strategy. Advanced Materials, 2020, 32, e2001243.	11.1	157
22	Highâ€Performance ZnO Transistors Processed Via an Aqueous Carbonâ€Free Metal Oxide Precursor Route at Temperatures Between 80–180 °C. Advanced Materials, 2013, 25, 4340-4346.	11.1	156
23	Hybrid Perovskite Thinâ€Film Photovoltaics: In Situ Diagnostics and Importance of the Precursor Solvate Phases. Advanced Materials, 2017, 29, 1604113.	11.1	155
24	Heterojunction oxide thin-film transistors with unprecedented electron mobility grown from solution. Science Advances, 2017, 3, e1602640.	4.7	148
25	Polymer Solar Cells with Efficiency >10% Enabled via a Facile Solutionâ€Processed Alâ€Doped ZnO Electron Transporting Layer. Advanced Energy Materials, 2015, 5, 1500204.	10.2	142
26	Highly Efficient Ruddlesden–Popper Halide Perovskite PA ₂ MA ₄ Pb ₅ 16 Solar Cells. ACS Energy Letters, 2018, 3, 1975-1982.	8.8	135
27	High Electron Mobility Thinâ€Film Transistors Based on Solutionâ€Processed Semiconducting Metal Oxide Heterojunctions and Quasiâ€Superlattices. Advanced Science, 2015, 2, 1500058.	5.6	134
28	Entanglement of Conjugated Polymer Chains Influences Molecular Selfâ€Assembly and Carrier Transport. Advanced Functional Materials, 2013, 23, 6024-6035.	7.8	131
29	Scalable Ambient Fabrication of High-Performance CsPbI2Br Solar Cells. Joule, 2019, 3, 2485-2502.	11.7	124
30	Centimeterâ€Sized Single Crystal of Twoâ€Dimensional Halide Perovskites Incorporating Straightâ€Chain Symmetric Diammonium Ion for Xâ€Ray Detection. Angewandte Chemie - International Edition, 2020, 59, 14896-14902.	7.2	124
31	Centimeterâ€Sized Single Crystals of Twoâ€Dimensional Hybrid Iodide Double Perovskite (4,4â€Difluoropiperidinium) ₄ AgBil ₈ for Highâ€Temperature Ferroelectricity and Efficient Xâ€Ray Detection. Advanced Functional Materials, 2021, 31, 2009457.	7.8	121
32	A New Method to Improve Poly(3-hexyl thiophene) (P3HT) Crystalline Behavior: Decreasing Chains Entanglement To Promote Orderâ^'Disorder Transformation in Solution. Langmuir, 2010, 26, 471-477.	1.6	110
33	40.1% Record Lowâ€Light Solarâ€Cell Efficiency by Holistic Trapâ€Passivation using Micrometerâ€Thick Perovskite Film. Advanced Materials, 2021, 33, e2100770.	11.1	110
34	Precursor Engineering for Ambientâ€Compatible Antisolventâ€Free Fabrication of Highâ€Efficiency CsPbl ₂ Br Perovskite Solar Cells. Advanced Energy Materials, 2020, 10, 2000691.	10.2	106
35	Vertical Phase Separation in Small Molecule:Polymer Blend Organic Thin Film Transistors Can Be Dynamically Controlled. Advanced Functional Materials, 2016, 26, 1737-1746.	7.8	98
36	Ionic Liquid Treatment for Highestâ€Efficiency Ambient Printed Stable Allâ€Inorganic CsPbl ₃ Perovskite Solar Cells. Advanced Materials, 2022, 34, e2106750.	11.1	97

Киі Zhao

#	Article	IF	CITATIONS
37	Large and Dense Organic–Inorganic Hybrid Perovskite CH ₃ NH ₃ PbI ₃ Wafer Fabricated by One-Step Reactive Direct Wafer Production with High X-ray Sensitivity. ACS Applied Materials & Interfaces, 2020, 12, 16592-16600.	4.0	94
38	Vapor-fumigation for record efficiency two-dimensional perovskite solar cells with superior stability. Energy and Environmental Science, 2018, 11, 3349-3357.	15.6	87
39	Reducing the confinement of PBDB-T to ITIC to improve the crystallinity of PBDB-T/ITIC blends. Journal of Materials Chemistry A, 2018, 6, 15610-15620.	5.2	86
40	In situ UV-visible absorption during spin-coating of organic semiconductors: a new probe for organic electronics and photovoltaics. Journal of Materials Chemistry C, 2014, 2, 3373.	2.7	82
41	Inch-sized high-quality perovskite single crystals by suppressing phase segregation for light-powered integrated circuits. Science Advances, 2021, 7, .	4.7	81
42	Indium Oxide Thin-Film Transistors Processed at Low Temperature via Ultrasonic Spray Pyrolysis. ACS Applied Materials & Interfaces, 2015, 7, 782-790.	4.0	79
43	Entanglements in marginal solutions: a means of tuning pre-aggregation of conjugated polymers with positive implications for charge transport. Journal of Materials Chemistry C, 2015, 3, 7394-7404.	2.7	75
44	Ultrastable Perovskite–Zeolite Composite Enabled by Encapsulation and Inâ€Situ Passivation. Angewandte Chemie - International Edition, 2020, 59, 23100-23106.	7.2	75
45	Dual Passivation of Perovskite and SnO ₂ for Highâ€Efficiency MAPbI ₃ Perovskite Solar Cells. Advanced Science, 2021, 8, 2001466.	5.6	72
46	Contactâ€Induced Nucleation in Highâ€Performance Bottomâ€Contact Organic Thin Film Transistors Manufactured by Largeâ€Area Compatible Solution Processing. Advanced Functional Materials, 2016, 26, 2371-2378.	7.8	71
47	<i>m</i> -Phenylenediammonium as a New Spacer for Dion–Jacobson Two-Dimensional Perovskites. Journal of the American Chemical Society, 2021, 143, 12063-12073.	6.6	71
48	Stable High-Performance Flexible Photodetector Based on Upconversion Nanoparticles/Perovskite Microarrays Composite. ACS Applied Materials & Interfaces, 2017, 9, 19176-19183.	4.0	70
49	Optimizing Morphology to Trade Off Charge Transport and Mechanical Properties of Stretchable Conjugated Polymer Films. Macromolecules, 2021, 54, 3907-3926.	2.2	70
50	Ambient blade coating of mixed cation, mixed halide perovskites without dripping: <i>in situ</i> investigation and highly efficient solar cells. Journal of Materials Chemistry A, 2020, 8, 1095-1104.	5.2	68
51	Metalâ€Free Halide Perovskite Single Crystals with Very Long Charge Lifetimes for Efficient Xâ€ray Imaging. Advanced Materials, 2020, 32, e2003353.	11.1	68
52	Large Leadâ€Free Perovskite Single Crystal for Highâ€Performance Coplanar Xâ€Ray Imaging Applications. Advanced Optical Materials, 2020, 8, 2000814.	3.6	67
53	Film Formation Control for High Performance Dion–Jacobson 2D Perovskite Solar Cells. Advanced Energy Materials, 2021, 11, 2002733.	10.2	62
54	Quasi Two-Dimensional Dye-Sensitized In ₂ O ₃ Phototransistors for Ultrahigh Responsivity and Photosensitivity Photodetector Applications. ACS Applied Materials & Interfaces, 2016, 8, 4894-4902.	4.0	61

#	Article	IF	CITATIONS
55	Synergistic Impact of Solvent and Polymer Additives on the Film Formation of Small Molecule Blend Films for Bulk Heterojunction Solar Cells. Advanced Energy Materials, 2015, 5, 1501121.	10.2	56
56	Toward Additiveâ€Free Smallâ€Molecule Organic Solar Cells: Roles of the Donor Crystallization Pathway and Dynamics. Advanced Materials, 2015, 27, 7285-7292.	11.1	56
57	The evidence of porcine hemagglutinating encephalomyelitis virus induced nonsuppurative encephalitis as the cause of death in piglets. PeerJ, 2016, 4, e2443.	0.9	52
58	Radio Frequency Coplanar ZnO Schottky Nanodiodes Processed from Solution on Plastic Substrates. Small, 2016, 12, 1993-2000.	5.2	48
59	Highly Luminescent Metalâ€Free Perovskite Single Crystal for Biocompatible Xâ€Ray Detector to Attain Highest Sensitivity. Advanced Materials, 2021, 33, e2102190.	11.1	46
60	Impact of the Solvation State of Lead Iodide on Its Two‧tep Conversion to MAPbI ₃ : An In Situ Investigation. Advanced Functional Materials, 2019, 29, 1807544.	7.8	45
61	Stable 2D Alternating Cation Perovskite Solar Cells with Power Conversion Efficiency >19% via Solvent Engineering. Solar Rrl, 2021, 5, 2100286.	3.1	45
62	Hybrid tandem solar cells with depleted-heterojunction quantum dot and polymer bulk heterojunction subcells. Nano Energy, 2015, 17, 196-205.	8.2	43
63	Porcine Hemagglutinating Encephalomyelitis Virus Activation of the Integrin α5β1-FAK-Cofilin Pathway Causes Cytoskeletal Rearrangement To Promote Its Invasion of N2a Cells. Journal of Virology, 2019, 93,	1.5	42
64	In‣itu Hot Oxygen Cleansing and Passivation for Allâ€Inorganic Perovskite Solar Cells Deposited in Ambient to Breakthrough 19% Efficiency. Advanced Functional Materials, 2021, 31, 2101568.	7.8	42
65	Spontaneous Construction of Multidimensional Heterostructure Enables Enhanced Hole Extraction for Inorganic Perovskite Solar Cells to Exceed 20% Efficiency. Advanced Energy Materials, 2022, 12, 2103007.	10.2	42
66	Highly efficient organic solar cells based on a robust room-temperature solution-processed copper iodide hole transporter. Nano Energy, 2015, 16, 458-469.	8.2	41
67	Roomâ€Temperature Partial Conversion of αâ€FAPbI ₃ Perovskite Phase via PbI ₂ Solvation Enables Highâ€Performance Solar Cells. Advanced Functional Materials, 2020, 30, 1907442.	7.8	41
68	Impact of Molecular Orientation and Spontaneous Interfacial Mixing on the Performance of Organic Solar Cells. Chemistry of Materials, 2015, 27, 5597-5604.	3.2	40
69	Crystallizationâ€Induced Phase Segregation Based on Doubleâ€Crystalline Blends of Poly(3â€hexylthiophene) and Poly(ethylene glycol)s. Macromolecular Rapid Communications, 2010, 31, 532-538.	2.0	38
70	Porcine Hemagglutinating Encephalomyelitis Virus Enters Neuro-2a Cells via Clathrin-Mediated Endocytosis in a Rab5-, Cholesterol-, and pH-Dependent Manner. Journal of Virology, 2017, 91, .	1.5	38
71	Ligand-Size Related Dimensionality Control in Metal Halide Perovskites. ACS Energy Letters, 2019, 4, 1830-1838.	8.8	38
72	Ligandâ€Anchoringâ€Induced Oriented Crystal Growth for Highâ€Efficiency Leadâ€Tin Perovskite Solar Cells. Advanced Functional Materials, 2022, 32, .	7.8	38

#	Article	IF	CITATIONS
73	Signatures of Quantized Energy States in Solutionâ€Processed Ultrathin Layers of Metalâ€Oxide Semiconductors and Their Devices. Advanced Functional Materials, 2015, 25, 1727-1736.	7.8	36
74	Solution Coating of Superior Largeâ€Area Flexible Perovskite Thin Films with Controlled Crystal Packing. Advanced Optical Materials, 2017, 5, 1700102.	3.6	34
75	Effective Phaseâ€Alignment for 2D Halide Perovskites Incorporating Symmetric Diammonium Ion for Photovoltaics. Advanced Science, 2021, 8, e2001433.	5.6	32
76	In Situ Study of Molecular Aggregation in Conjugated Polymer/Elastomer Blends toward Stretchable Electronics. Macromolecules, 2022, 55, 297-308.	2.2	30
77	Microstructure and lattice strain control towards high-performance ambient green-printed perovskite solar cells. Journal of Materials Chemistry A, 2021, 9, 13297-13305.	5.2	29
78	Metalâ€Free Organic Halide Perovskite: A New Class for Next Optoelectronic Generation Devices. Advanced Energy Materials, 2021, 11, 2003331.	10.2	29
79	Formamidinium-based Ruddlesden–Popper perovskite films fabricated <i>via</i> two-step sequential deposition: quantum well formation, physical properties and film-based solar cells. Energy and Environmental Science, 2022, 15, 1144-1155.	15.6	27
80	Induction of Atypical Autophagy by Porcine Hemagglutinating Encephalomyelitis Virus Contributes to Viral Replication. Frontiers in Cellular and Infection Microbiology, 2017, 7, 56.	1.8	25
81	Carrier Generation Engineering toward 18% Efficiency Organic Solar Cells by Controlling Film Microstructure. Advanced Energy Materials, 2022, 12, .	10.2	25
82	Centimeter-Sized 2D Perovskitoid Single Crystals for Efficient X-ray Photoresponsivity. Chemistry of Materials, 2022, 34, 1699-1709.	3.2	24
83	Solvent-dependent self-assembly and ordering in slow-drying drop-cast conjugated polymer films. Journal of Materials Chemistry C, 2015, 3, 9842-9848.	2.7	23
84	Centimeterâ€ s ized Molecular Perovskite Crystal for Efficient Xâ€Ray Detection. Advanced Functional Materials, 2021, 31, 2100691.	7.8	22
85	Direct–Indirect Transition of Pressurized Two-Dimensional Halide Perovskite: Role of Benzene Ring Stack Ordering. Journal of Physical Chemistry Letters, 2019, 10, 5687-5693.	2.1	20
86	miR-142-5p Disrupts Neuronal Morphogenesis Underlying Porcine Hemagglutinating Encephalomyelitis Virus Infection by Targeting Ulk1. Frontiers in Cellular and Infection Microbiology, 2017, 7, 155.	1.8	19
87	Efficient Hybrid Mixedâ€lon Perovskite Photovoltaics: In Situ Diagnostics of the Roles of Cesium and Potassium Alkali Cation Addition. Solar Rrl, 2020, 4, 2000272.	3.1	19
88	Efficient Eco-Friendly Flexible X-ray Detectors Based on Molecular Perovskite. Nano Letters, 2022, 22, 5973-5981.	4.5	19
89	Ulk1 Governs Nerve Growth Factor/TrkA Signaling by Mediating Rab5 GTPase Activation in Porcine Hemagglutinating Encephalomyelitis Virus-Induced Neurodegenerative Disorders. Journal of Virology, 2018, 92, .	1.5	18
90	Perovskite Solar Cells toward Eco-Friendly Printing. Research, 2021, 2021, 9671892.	2.8	18

#	Article	IF	CITATIONS
91	Inch-size Cs ₃ Bi ₂ I ₉ polycrystalline wafers with near-intrinsic properties for ultralow-detection-limit X-ray detection. Journal of Materials Chemistry C, 2022, 10, 6665-6672.	2.7	18
92	Waterâ€Resistant Leadâ€Free Perovskitoid Single Crystal for Efficient Xâ€Ray Detection. Advanced Functional Materials, 2022, 32, .	7.8	18
93	Hybrid Modulationâ€Doping of Solutionâ€Processed Ultrathin Layers of ZnO Using Molecular Dopants. Advanced Materials, 2016, 28, 3952-3959.	11.1	16
94	ATN-161 reduces virus proliferation in PHEV-infected mice by inhibiting the integrin α5β1-FAK signaling pathway. Veterinary Microbiology, 2019, 233, 147-153.	0.8	16
95	Blending Donors with Different Molecular Weights: An Efficient Strategy to Resolve the Conflict between Coherence Length and Intermixed Phase in Polymer/Nonfullerene Solar Cells. Small, 2022, 18, e2103804.	5.2	16
96	Carrier Transport Enhancement in Conjugated Polymers through Interfacial Self-Assembly of Solution-State Aggregates. ACS Applied Materials & Interfaces, 2016, 8, 19649-19657.	4.0	15
97	Role of Alkali-Metal Cations in Electronic Structure and Halide Segregation of Hybrid Perovskites. ACS Applied Materials & Interfaces, 2020, 12, 34402-34412.	4.0	15
98	Sequential Formation of Tunableâ€Bandgap Mixedâ€Halide Leadâ€Based Perovskites: In Situ Investigation and Photovoltaic Devices. Solar Rrl, 2021, 5, .	3.1	15
99	The PERK/PKR-eIF2α Pathway Negatively Regulates Porcine Hemagglutinating Encephalomyelitis Virus Replication by Attenuating Global Protein Translation and Facilitating Stress Granule Formation. Journal of Virology, 2022, 96, JVI0169521.	1.5	15
100	Ionâ€Accumulationâ€Induced Charge Tunneling for High Gain Factor in P–I–Nâ€Structured Perovskite CH ₃ NH ₃ PbI ₃ Xâ€Ray Detector. Advanced Materials Technologies, 2022, 7, 2100908.	3.0	15
101	Gene-expression patterns in the cerebral cortex of mice infected with porcine haemagglutinating encephalomyelitis virus detected using microarray. Journal of General Virology, 2014, 95, 2192-2203.	1.3	13
102	Genomic characterization of two Orf virus isolates from Jilin province in China. Virus Genes, 2019, 55, 490-501.	0.7	13
103	MiR-10a-5p-Mediated Syndecan 1 Suppression Restricts Porcine Hemagglutinating Encephalomyelitis Virus Replication. Frontiers in Microbiology, 2020, 11, 105.	1.5	13
104	Orf Virus ORF120 Protein Positively Regulates the NF-κB Pathway by Interacting with G3BP1. Journal of Virology, 2021, 95, e0015321.	1.5	13
105	Phase Separation in Poly(9,9â€dioctylfluorene)/Poly(methyl methacrylate) Blends. Macromolecular Chemistry and Physics, 2010, 211, 313-320.	1.1	12
106	miR-21a-5p Contributes to Porcine Hemagglutinating Encephalomyelitis Virus Proliferation via Targeting CASK-Interactive Protein1 In vivo and vitro. Frontiers in Microbiology, 2017, 8, 304.	1.5	12
107	Centimeterâ€Sized Single Crystal of Twoâ€Dimensional Halide Perovskites Incorporating Straightâ€Chain Symmetric Diammonium Ion for Xâ€Ray Detection. Angewandte Chemie, 2020, 132, 15006-15012.	1.6	11
108	Genomic characterization and pathogenicity of a porcine hemagglutinating encephalomyelitis virus strain isolated in China. Virus Genes, 2018, 54, 672-683.	0.7	10

#	Article	IF	CITATIONS
109	An Experimental Model of Neurodegenerative Disease Based on Porcine Hemagglutinating Encephalomyelitis Virus–Related Lysosomal Abnormalities. Molecular Neurobiology, 2020, 57, 5299-5306.	1.9	10
110	Controlling Phase Transition toward Future Low-Cost and Eco-friendly Printing of Perovskite Solar Cells. Journal of Physical Chemistry Letters, 2022, 13, 6503-6513.	2.1	9
111	Structural and Functional Insights into Metal-Free Perovskites. Journal of Physical Chemistry Letters, 2022, 13, 5168-5178.	2.1	8
112	The matrix protein of vesicular stomatitis virus inhibits host-directed transcription of target genes via interaction with the TFIIH subunit p8. Veterinary Microbiology, 2017, 208, 82-88.	0.8	7
113	Ultrastable Perovskite–Zeolite Composite Enabled by Encapsulation and Inâ€Situ Passivation. Angewandte Chemie, 2020, 132, 23300-23306.	1.6	7
114	Control of Phase Separation and Crystallization for <scp>Highâ€Efficiency</scp> and <scp>Mechanically Deformable</scp> Organic Solar Cells. Energy and Environmental Materials, 2023, 6, .	7.3	6
115	Development of a lateral flow immunochromatographic assay for the rapid diagnosis of Orf virus infections. Journal of Virological Methods, 2016, 236, 10-17.	1.0	5
116	EIF3i affects vesicular stomatitis virus growth by interacting with matrix protein. Veterinary Microbiology, 2017, 212, 59-66.	0.8	5
117	Transition-Metal-Free Synthesis of Aryl Trifluoromethyl Thioethers through Indirect Trifluoromethylthiolation of Sodium Arylsulfinate with TMSCF ₃ . Organic Letters, 2021, 23, 6982-6986.	2.4	5
118	Processing of Lead Halide Perovskite Thin Films Studied with In-Situ Real-Time X-ray Scattering. ACS Applied Materials & Interfaces, 2022, 14, 26315-26326.	4.0	5
119	miR-142a-3p promotes the proliferation of porcine hemagglutinating encephalomyelitis virus by targeting Rab3a. Archives of Virology, 2020, 165, 345-354.	0.9	4
120	Porcine haemagglutinating encephalomyelitis virus deactivates transcription factor IRF3 and limits type I interferon production. Veterinary Microbiology, 2021, 252, 108918.	0.8	4
121	Porcine Hemagglutinating Encephalomyelitis Virus Triggers Neural Autophagy Independently of ULK1. Journal of Virology, 2021, 95, e0085121.	1.5	4
122	Perovskite Photovoltaics: Hybrid Perovskite Thinâ€Film Photovoltaics: In Situ Diagnostics and Importance of the Precursor Solvate Phases (Adv. Mater. 2/2017). Advanced Materials, 2017, 29, .	11.1	3
123	Porcine hemagglutinating encephalomyelitis virus induces atypical autophagy via opposite regulation of expression and nuclear translocation of transcription factor EB. Veterinary Microbiology, 2021, 255, 109015.	0.8	3
124	Cell-surface glycans act as attachment factors for porcine hemagglutinating encephalomyelitis virus. Veterinary Microbiology, 2022, 265, 109315.	0.8	3
125	Evidence of Microglial Immune Response Following Coronavirus PHEV Infection of CNS. Frontiers in Immunology, 2021, 12, 804625.	2.2	3

Thin Film Transistors: Contact-Induced Nucleation in High-Performance Bottom-Contact Organic Thin Film Transistors Manufactured by Large-Area Compatible Solution Processing (Adv. Funct. Mater.) Tj ETQq0 0 0 rgBT.#Overloc 10 Tf 50

Киі Zhao

#	Article	IF	CITATIONS
127	Host factor cyclophilin B affects Orf virus replication by interacting with viral ORF058 protein. Veterinary Microbiology, 2021, 258, 109099.	0.8	2
128	Roles of Organic Ligands in Ambient Stability of Layered Halide Perovskites. ACS Applied Materials & Interfaces, 2022, 14, 33085-33093.	4.0	2
129	Editorial: Polymer Solar Cells: Molecular Design and Microstructure Control. Frontiers in Chemistry, 2020, 8, 697.	1.8	1
130	In Situ Investigation and Photovoltaic Devices: Sequential Formation of Tunable-Bandgap Mixed-Halide Lead-based Perovskites. , 0, , .		1
131	Polymers for new energy technology. Journal of Polymer Science, 2022, 60, 863-864.	2.0	1
132	Microtubule depolymerization limits porcine betacoronavirus PHEV replication. Veterinary Microbiology, 2022, 269, 109448.	0.8	0